SI Appendix

Distinct roles of resident and non-resident macrophages in non-ischemic cardiomyopathy

Xudong Liao[a,*], Yuyan Shen[a], Rongli Zhang[a], Keiki Sugi[a], Neelakantan T. Vasudevan[a], M. Amer Alaiti[a], David R. Sweet[a], Lin Zhou[b], Yulan Qing[c], Stanton L. Gerson[c], Chen Fu[d], Anthony Wynshaw-Boris[d], Rui Hu[e], Martin A. Schwartz[e], Hisashi Fujioka[f], Brian Richardson[g], Mark J. Cameron[g], Hiroki Hayashi[h], Jonathan S. Stamler[h], and Mukesh K. Jain[a,*]

[a] Case Cardiovascular Research Institute, Case Western Reserve University School of Medicine, Harrington Heart and Vascular Institute, University Hospitals Cleveland Medical Center, Cleveland, Ohio 44106, USA.
[b] Department of Cardiology, Tongji Hospital of Tongji University, Shanghai 20065, China.
[c] Case Comprehensive Cancer Center, National Center for Regenerative Medicine, Seidman Cancer Center, University Hospitals Cleveland Medical center and Case Western Reserve University, Cleveland, Ohio 44106, USA.
[d] Department of Genetics and Genome Sciences, Case Western Reserve University School of Medicine, Cleveland, Ohio 44106, USA.
[e] Yale Cardiovascular Research Center, Yale University, New Heaven, CT 06511, USA.
[f] Electron Microscopy Core Facility, Case Western Reserve University School of Medicine, Cleveland, Cleveland, Ohio 44106, USA.
[g] Department of Epidemiology and Biostatistics, Case Western Reserve University, Cleveland, Ohio 44106, USA
[h] Institute of Translational Molecular Medicine, Case Western Reserve University School of Medicine, Harrington Heart and Vascular Institute, University Hospitals Cleveland Medical Center, Cleveland, Ohio 44106, USA.

***Corresponding Author:**

Mukesh K. Jain, MD
2103 Cornell Road, Room 4537
Cleveland, OH 44106-7290
Tel: 216-368-3607
Fax: 216-368-0556
Email: mukesh.jain2@case.edu

Xudong Liao, PhD
2103 Cornell Road, WRB-4503
Cleveland, OH 44106
Tel: 216-368-0591
Fax: 216-368-2591
Email: xudong.liao@case.edu

Materials and Methods

Cell culture

Mouse thioglycollate-elicited peritoneal macrophages (PM) and mouse bone marrow derived macrophages (BMDM) were prepared as described previously (1).

Animals

Mice with myeloid-specific deficiency of Klf4 (Lyz2-Cre:Klf4$^{fl/fl}$, K4-cKO) or IL4Ra (Lyz2-Cre:IL4Ra$^{fl/fl}$, IL4Ra-cKO) were described previously (1, 2). The Lyz2-Cre line (Cre) was used as genetic control (1). WT C57BL/6J (B6-CD45.2), B6-CD45.1 and CCR2-KO mice were purchased from Jackson laboratory (3, 4). All mice are on a C57BL/6J background. Mice were housed in a temperature- and humidity-controlled specific pathogen–free facility with a 12-hour-light/dark cycle and ad libitum access to water and standard laboratory rodent chow.

CD45.1-CD45.2 chimera mice

Partial bone marrow transplantation was performed with B6-CD45.2 as recipient and B6-CD45.1 as donor. The rear part of recipient CD45.2 mice were exposed to lethal dose gamma ray while chest and head area was shielded by lead block. After irradiation, two million CD45.1 bone marrow cells were transplanted via tail vein injection and recipients were allowed to recover for 2 months before blood test for CD45.1 cells. Blood (50 uL) was drawn from tail and subjected to immunostaining with fluorescent antibodies for CD11b, CD45.1, and CD45.2 for FACS analysis. Mice with >50% CD45.1 myeloid cells were used for TAC models.

Macrophage depletion, CCR2 blockade and neutrophil depletion

Macrophage depletion was achieved by injection (i.v.) of Clodronate liposomes at 500 ug/kg on every other day, starting from 1-day before or 14-day after cardiac surgery as indicated in specific experiments. PBS-containing liposomes were used as vehicle control (Veh). Clodronate liposomes and control liposomes were obtained from the nonprofit Consortium Foundation Clodronate Liposomes. To inhibit monocyte trafficking in vivo, RS-504393 was dissolved in DMSO, diluted 1:20 in PBS and administrated at 2 mg/kg twice daily by oral gavage (5), starting from 1-

day before or 14-day after cardiac surgery as indicated in specific experiments. PBS with 5% DMSO was used as vehicle control.

Neutrophil depletion was achieved by injection (i.p.) of anti-Ly6G antibody (clone 1A8, Bio X Cell). Total 100 ug antibody in 100 ul PBS was injected per mouse (body weight 25-30g). To maintain stable depletion, mice were injected every other day. Normal rat IgG was used as control.

Pressure overload hypertrophy studies

Transverse aortic constriction (TAC) model and echocardiography were performed as described previously (6). Mice were anaesthetized by ketamine xylazine cocktail (100 uL i.p.) for TAC surgery to reduce aorta diameter to 27-gague. Buprenorphine was administrated daily (i.p.) for first 5-days post-TAC. Blood pressure gradient across ligation site was confirmed by Doppler echography. For echocardiography, mice were anaesthetized by inhalation of 1% isoflurane vaporized in 100% oxygen. LV function was recorded at parasternal short axis view in B-mode and M-mode on a VEVO 770 High-Resolution In Vivo Micro-Imaging System (VisualSonics). ECHO data were recorded at steady heart rate above 500 bpm. LV function was calculated as ejection fraction (EF) or fractional shortening (FS).

Flow cytometry

Peritoneal macrophages were collected as described previously (1). Cardiac macrophages were gated from whole heart cells using surface antibodies ($CD45^+CD11b^+F4/80^+Ly6G^-CD64^+$). Mouse heart is perfused, excised, minced, digested with Type I collagenase, mechanically disrupted and filtered through 70 μm cell strainer to get single cell suspension (7). Cells are collected by centrifugation, subjected to live-death dye and surface antibody staining, and analyzed by flow cytometry. Cells were also sorted by flow cytometry to collect cardiac macrophages. For Ki-67 staining, surface stained cells were fixed and permeabilized by the FIX PERM Cell Permeabilization Kit (ThermoFisher), and further stained with anti-Ki-67 antibody. DNA was stained with Hoechst 33342. For monocyte analysis, blood was collected from inferior vena cava (IVC), bone marrow cells were flush from femurs, and spleen was mashed on a 40-μm cell strainer. After RBC lysis, cells were stained with surface antibodies and analyzed by FACS. Monocytes were gated as $CD115^+CD11b^+$ population and further gated for CX3CR1, Ly6C and CCR2 to distinguish classic vs.$^-$ non-classic monocytes.

In vivo BrdU pulse labeling studies

To assess local proliferation of cardiac resident macrophages, animals were injected (*i.p.*) with 2 mg BrdU and pulse labelled for 2 hours before harvest. During this 2-hour period, BrdU-labeled bone marrow cells have not been released into circulation, so that only local proliferating cells will be labeled as BrdU positive (8). The hearts were digested to single cell suspension and stained for cell surface markers as above. The BD Pharmingen™ APC BrdU Flow Kit (BD Sciences, 552598) was used to detect BrdU-labelled cells. In brief, surface stained cells were fixed and permeabilized using BD Cytofix/Cytoperm buffer and Cytoperm Permeabilization Plus buffer; digested with DNase I to expose BrdU antigen, stained with fluorescent APC-conjugated anti-BrdU antibody and analyzed using a BD LSR-II flow cytometer. DNA was stained with Hoechst 33342 for cycle analysis.

Histology

Cardiac tissue samples were fixed in 10% neutralized formalin and embedded with paraffin following standard protocol. Fibrosis was visualized using Picrosirius Red Stain Kit (Polysciences, Inc.) or Gomori's Trichrome staining kit (Sigma) (6). To determine cell death in the myocardium, TUNEL staining was performed with the Peroxidase-based or Fluorescein-based ApopTag In Situ Apoptosis Detection Kit (Millipore, S7100, S7110) following manufacturer's protocol (9). In fluorescent TUNEL staining, heart sections were double stained with anti-cardiac-actin (Sigma, A9357) primary antibody and Alexa Fluor 594-conjugated goat-anti-mouse-IgG secondary antibody (ThermoFisher) to visualize cardiomyocytes (5). To determine apoptosis, paraffin-embedded heart sections were stained with anti-Cleaved Caspase-3 (Asp175) antibody using the SignalStain® Apoptosis (Cleaved Caspase-3) IHC Detection Kit (Cell Signaling Technology, 12692S). Capillary staining was performed in cryopreserved heart sections using anti-CD31 primary antibody (1:50, BD 553370) and Alexa Fluor 594-conjugated goat-anti-rat-IgG secondary antibody (ThermoFisher). Cardiomyocyte cross sectional area was determined by staining with Alexa Fluor 5904-conjugated Wheat Germ Agglutinin (WGA) (ThermoFisher). Microscopic images were analyzed using NIH ImageJ software for quantification and channel overlay.

Transmission electron microscopy

Small pieces of tissue from the LV free wall were fixed by sequential immersion in triple aldehyde-

DMSO, ferrocyanide-reduced osmium tetroxide, and acidified uranyl acetate; dehydrated in ascending concentrations of ethanol; passed through propylene oxide; and embedded in Poly/Bed resin (Polysciences Inc., 21844-1). Thin sections were sequentially stained with acidified uranyl acetate, followed by a modification of Sato's triple lead stain, and examined with a JEOL 1200EX electron microscope (10).

RNA extraction and qPCR

Tissue samples were homogenized in QIAzol lysis reagent (Qiagen, 79306) with a TissueLyser (Qiagen). Cell samples were directly dissolved in QIAzol lysis reagent. Total RNA was extracted, treated with DNase I (Life Technologies, 18068015), purified using the RNeasy MinElute Cleanup Kit (Qiagen, 74204). The Qiagen RNeasy Micro Kit was used to extract RNA from small amount of FACS-sorted cells (5,000-10,000 cells). RNA was reverse transcribed to complementary DNA using the iScript Reverse Transcription Kit (Bio-Rad, 170-8841). Quantitative real-time PCR (qPCR) was performed with either the TaqMan method (Roche Universal ProbeLibrary System) or the SYBR green method on a ViiA 7 Real-Time PCR System (Applied Biosystems). Relative expression was calculated using the ΔΔCt method with normalization to Gapdh.

RNA-seq studies

For RNASeq, libraries were prepared using the Illumina TruSeq Stranded Total RNA Sample Preparation kit according to the manufacturer's protocol. 50 bp singled-end sequencing was performed on pooled libraries in groups of three using an Illumina HiSeq 2500. Sequencing reads generated from the Illumina platform were assessed for quality using FastQC. The reads were then trimmed for adapter sequences using TrimGalore. For RNASeq, reads that passed quality control were then aligned to rn6 using TOPHAT (11). The TOPHAT results were then analyzed for differential expression using cufflinks to generate the fragments per kilobase of exon per million fragments mapped (FPKM) for each gene (12). Differential genes were identified using a significance cutoff of $q < 0.005$ and fold change>1.5. These genes were then subjected to further analysis. Gene Ontology (GO) Enrichment Analysis was performed with the DAVID Bioinformatics Resources 6.8 (13, 14). RNA-seq data are deposited at Gene Expression Omnibus (GSE107016).

Statistics

Results are presented as mean ± SEM. Two-tailed Student's t test was used to compare the differences between two groups. One-way ANOVA and Bonferroni post-test was used for multiple comparisons. Two-way ANOVA and Bonferroni post-test was used for comparison between data curves. Significance between survival curves was determined by Log-rank test. Statistical significance was defined as $P < 0.05$. Statistics was performed using Prism 7 software.

Reference cited:

1. Liao X*, et al.* (2011) Kruppel-like factor 4 regulates macrophage polarization. *J Clin Invest* 121(7):2736-2749.
2. Nguyen KD*, et al.* (2011) Alternatively activated macrophages produce catecholamines to sustain adaptive thermogenesis. *Nature* 480(7375):104-108.
3. Janowska-Wieczorek A*, et al.* (2001) Platelet-derived microparticles bind to hematopoietic stem/progenitor cells and enhance their engraftment. *Blood* 98(10):3143-3149.
4. Boring L*, et al.* (1997) Impaired monocyte migration and reduced type 1 (Th1) cytokine responses in C-C chemokine receptor 2 knockout mice. *J Clin Invest* 100(10):2552-2561.
5. Lavine KJ*, et al.* (2014) Distinct macrophage lineages contribute to disparate patterns of cardiac recovery and remodeling in the neonatal and adult heart. *Proc Natl Acad Sci U S A* 111(45):16029-16034.
6. Liao X*, et al.* (2015) Kruppel-like factor 4 is critical for transcriptional control of cardiac mitochondrial homeostasis. *J Clin Invest* 125(9):3461-3476.
7. Sangwung P*, et al.* (2017) KLF2 and KLF4 control endothelial identity and vascular integrity. *JCI Insight* 2(4):e91700.
8. Epelman S*, et al.* (2014) Embryonic and adult-derived resident cardiac macrophages are maintained through distinct mechanisms at steady state and during inflammation. *Immunity* 40(1):91-104.
9. Liao X*, et al.* (2010) Kruppel-like factor 4 regulates pressure-induced cardiac hypertrophy. *J Mol Cell Cardiol* 49(2):334-338.
10. Fujioka H, Tandler B, Haldar SM, Jain MK, & Hoppel CL (2013) String mitochondria in mouse soleus muscle. *Microsc Res Tech* 76(3):237-241.
11. Trapnell C, Pachter L, & Salzberg SL (2009) TopHat: discovering splice junctions with RNA-Seq. *Bioinformatics* 25(9):1105-1111.
12. Trapnell C*, et al.* (2010) Transcript assembly and quantification by RNA-Seq reveals unannotated transcripts and isoform switching during cell differentiation. *Nat Biotechnol* 28(5):511-515.
13. Huang da W, Sherman BT, & Lempicki RA (2009) Systematic and integrative analysis of large gene lists using DAVID bioinformatics resources. *Nat Protoc* 4(1):44-57.
14. Huang da W, Sherman BT, & Lempicki RA (2009) Bioinformatics enrichment tools: paths toward the comprehensive functional analysis of large gene lists. *Nucleic Acids Res* 37(1):1-13.

Supplementary Figures

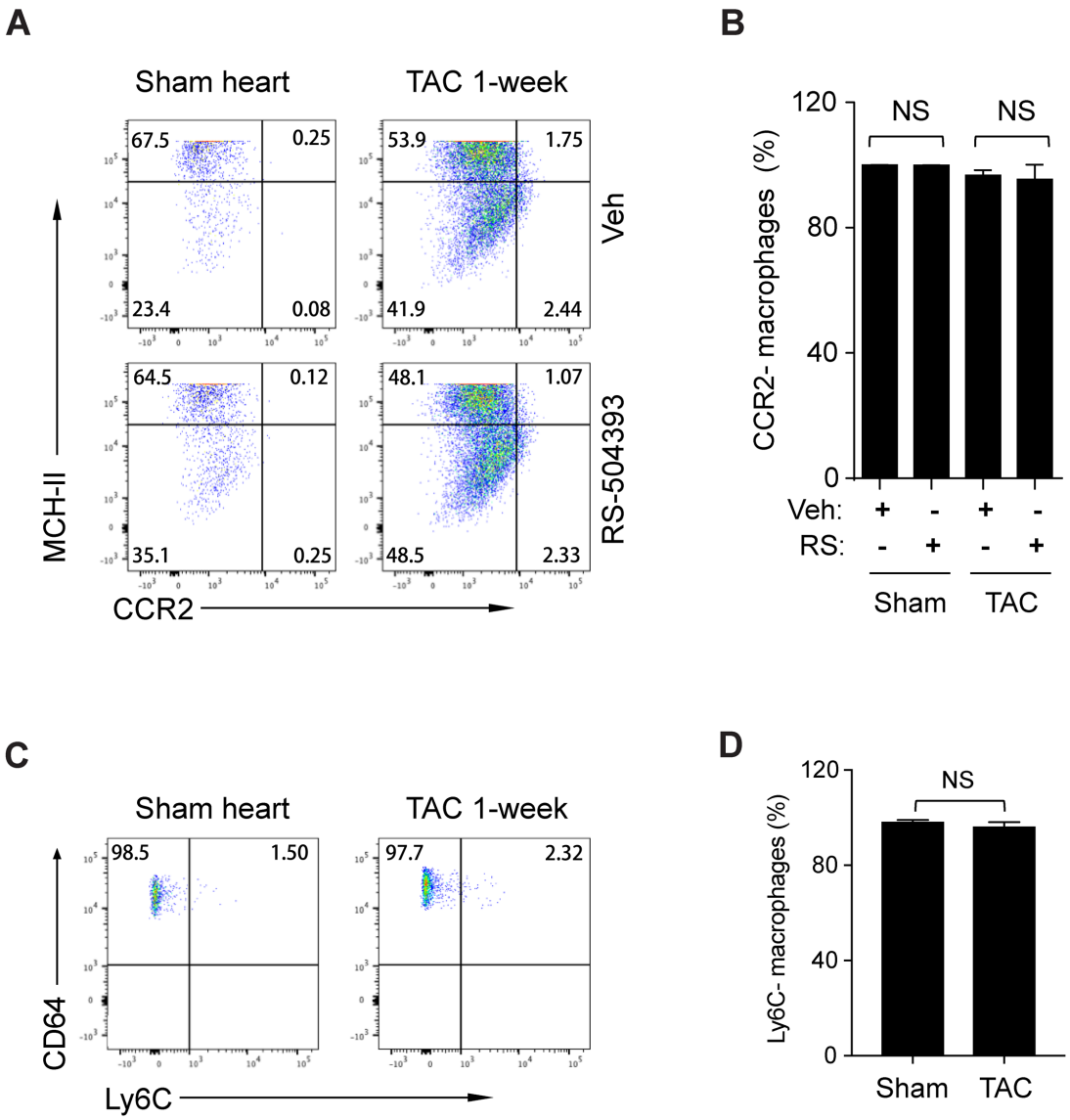

Figure S1. TAC did not induce significant monocyte infiltration in early-phase POH.

(A) FACS analysis of cardiac macrophages. MHC-II and CCR2 were plotted to show resident macrophages. (B) The CCR2^{-} resident macrophages remained as >90% after TAC, indicating no significant infiltration of CCR2^{+} monocytes at 1-week post-TAC. RS-504393 (RS) dissolved in PBS+5% DMSO was administrated by oral gavage in one set of animals to block CCR2-mediated chemotaxis. PBS+5%DMSO was used as vehicle (Veh) control. (C&D) Majority of cardiac macrophages are CD64^{+}Ly6C^{-} before and after 1-week TAC. n=5.

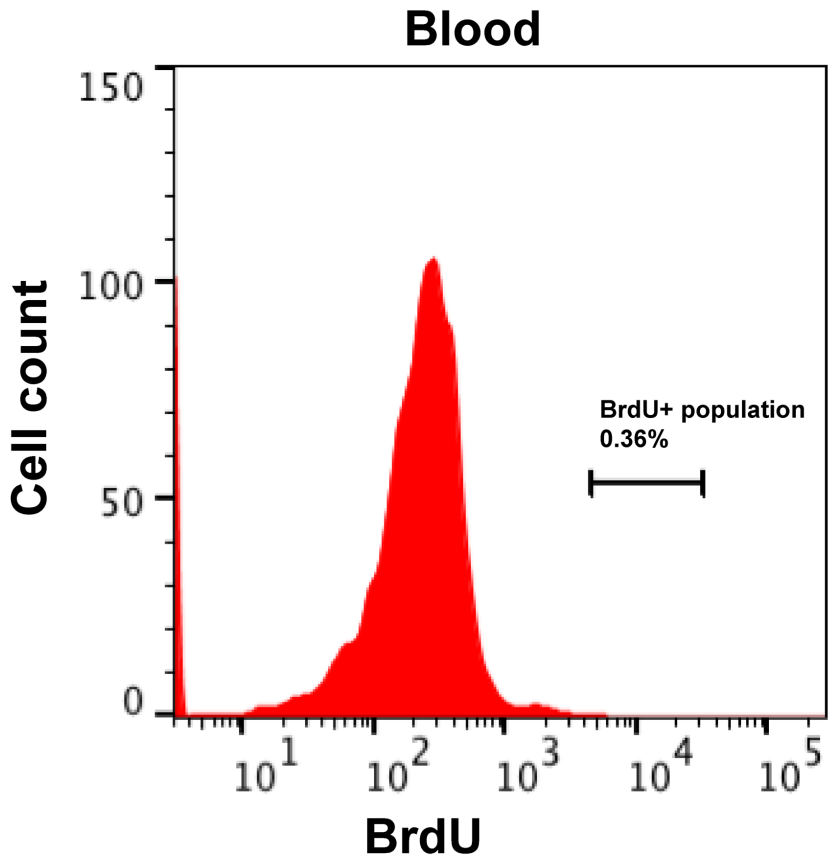

Figure S2. Two-hour BrdU pulse-labeling.

Blood cells were not labelled by BrdU within two hours of BrdU injection. BrdU incorporation into DNA was detected by APC-conjugated anti-BrdU antibody using FACS.

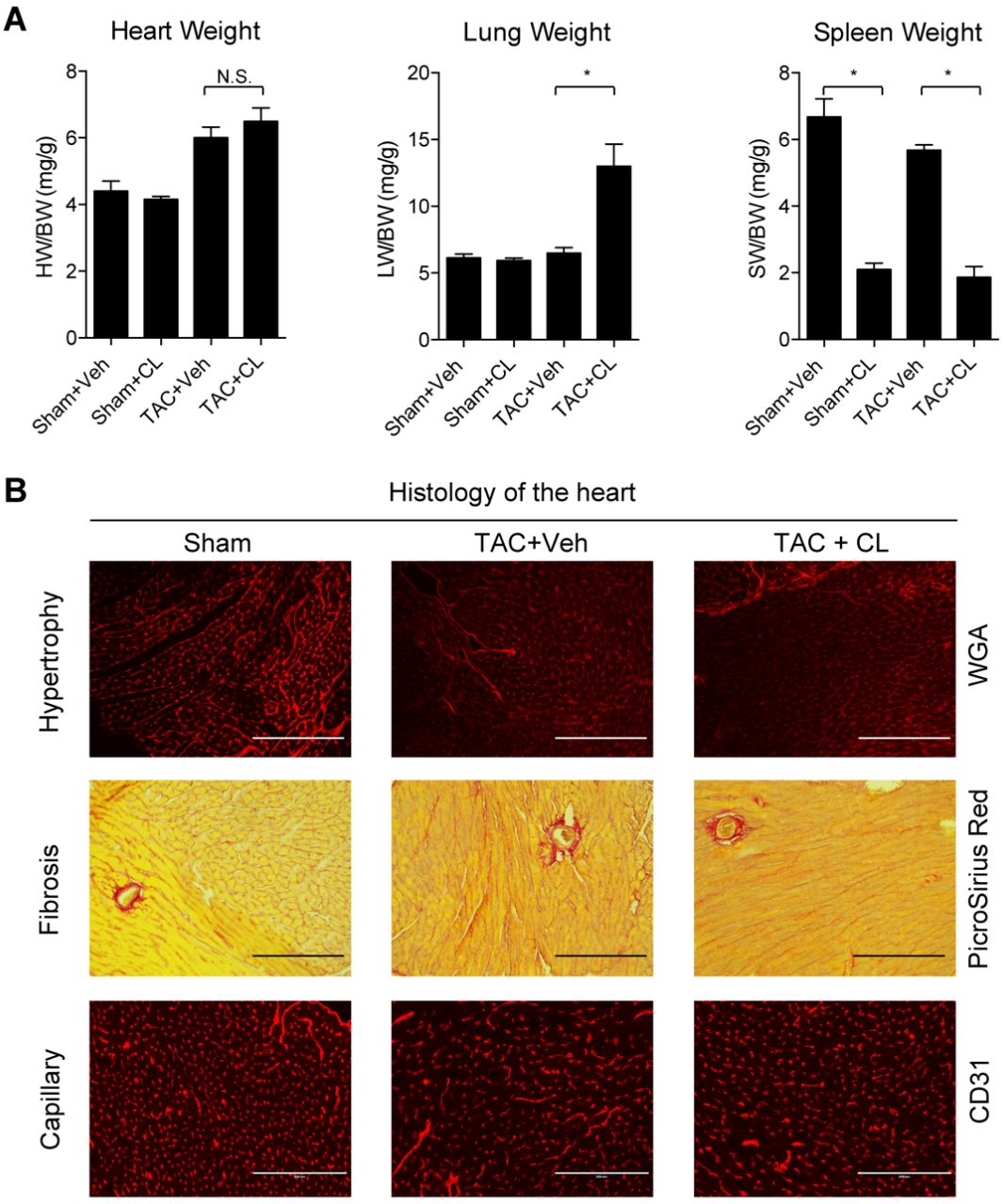

Figure S3. Clodronate liposome (CL)-mediated macrophage depletion.

(A) Organs from mice receiving 3 injections of control PBS-containing liposomes (Veh) and CL-containing liposomes (CL). Surgery was performed 1-day after first injection. Organ weight (in mg) was normalized to body weight (BW, in gram). HW: heart weight. LW: lung weight. SW: spleen weight. n=5, *p<0.05. (B) Histology of hearts after 4-day TAC and 3 injections of liposomes (Veh or CL). Cardiac hypertrophy was assessed by WGA staining. Fibrosis was assessed by PicoSirus Red staining. Collagen was stained in red. Myocardial capillary density was assessed by CD31 staining. Scale bar indicates 200 μm. All tissue samples were assessed at 4-day post-TAC (and after 3 injections).

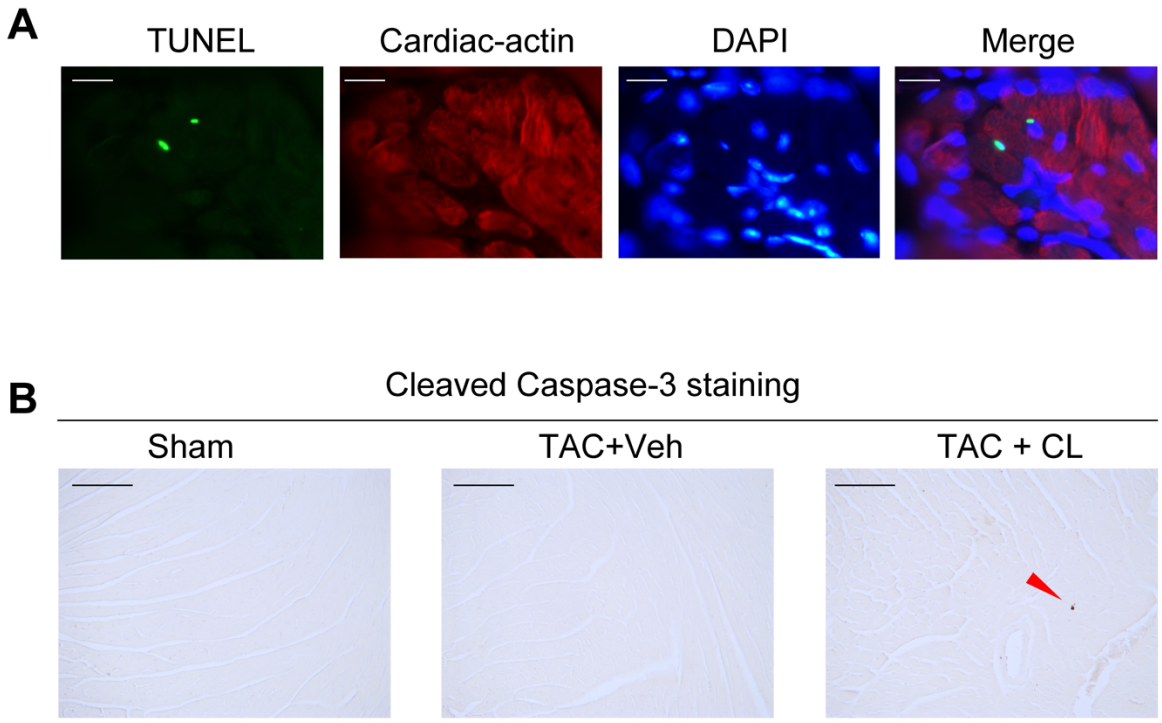

Figure S4. TAC induced non-apoptotic death of cardiomyocytes in macrophage-depletd (CL) heart.

(A) Fluorescent TUNEL staining coupled with anti-cardiac actin immunostaining. Green: TUNEL signal (dead nuclei). Red: cardiac actin. Blue: DAPI. Scale bar indicates 20 μm. (B) Immunostaining for cleaved Caspase 3 in the myocardium. Brown (DAB-positive) cells were highlighted with red arrow head. Scale bar indicates 100 μm. All tissue samples were assessed at 4-day post-TAC (and after 3 injections).

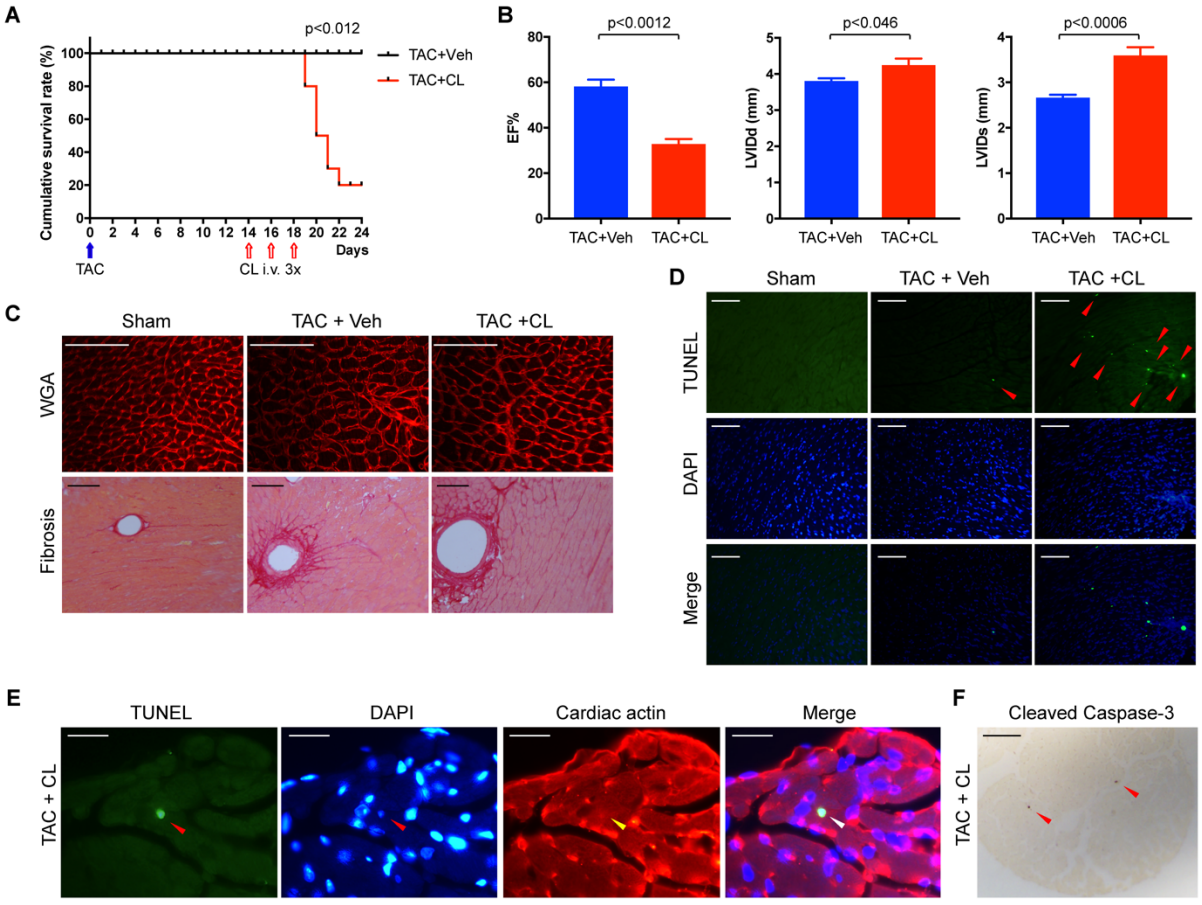

Figure S5. Macrophage depletion (CL) after 2 weeks of TAC induced quick transition to heart failure and death.

(A) Post-TAC survival rates. Blue arrow indicates time of TAC and red arrows indicate time of liposome injections. P value was calculated from Log-rank test. n=10 in each group. Veh: PBS liposomes; CL: Clodronate liposomes. (B) Echocardiography. *p<0.05 by t test. n=5. (C) Cardiomyocyte hypertrophy (WGA staining) and fibrosis (Sirius Red staining). Scale bar indicates 100 μm. (D) Cell death in the myocardium assessed by TUNEL staining. Scale bar indicates 100 μm. (E) Cardiac actin and TUNEL double staining confirmed cardiomyocyte death in TAC+CL heart. Scale bar indicates 25 μm. (F) Cleaved Caspase-3 staining showing very few apoptotic cells. Scale bar indicates 200 μm. Arrow heads indicate dead cells.

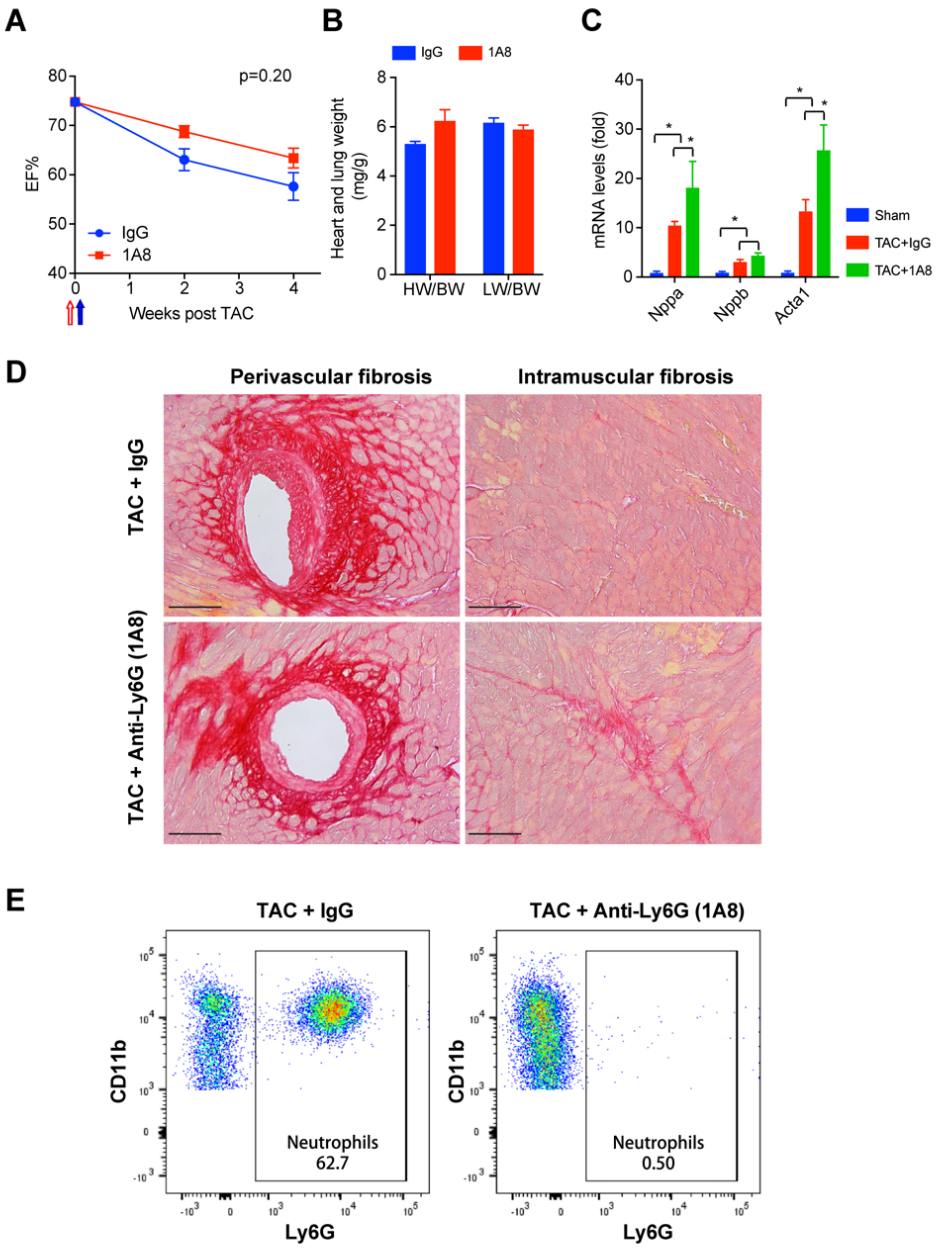

Figure S6. Depletion of neutrophils exhibited little effect on POH.

(A) LV function assessed by serial echocardiography. IgG: control antibody. 1A8: anti-Ly6G antibody, clone 1A8. Arrows: Antibody i.p. injection (red arrow) was started 1-day before TAC (blue arrow) and kept for 4 weeks during TAC. P value shown as P (treatment*time) calculated from Two-Way ANOVA. (B) heart weight (HW)and lung weight (LW) after 4-week TAC, normalized to body weight (BW). n=5. (C) Expression of hypertrophy marker genes (Nppa, Nppb and Acta1) in the heart after 4-week TAC. $P<0.05$ by t test with Bonferroni correction. n=5. (D) Fibrosis assessed by PicoSirus Red staining. Collagen was stained in red. Perivascular and intramuscular areas were shown. Scale bar indicates 100 μm (E) Neutrophil depletion was confirmed by FACS.

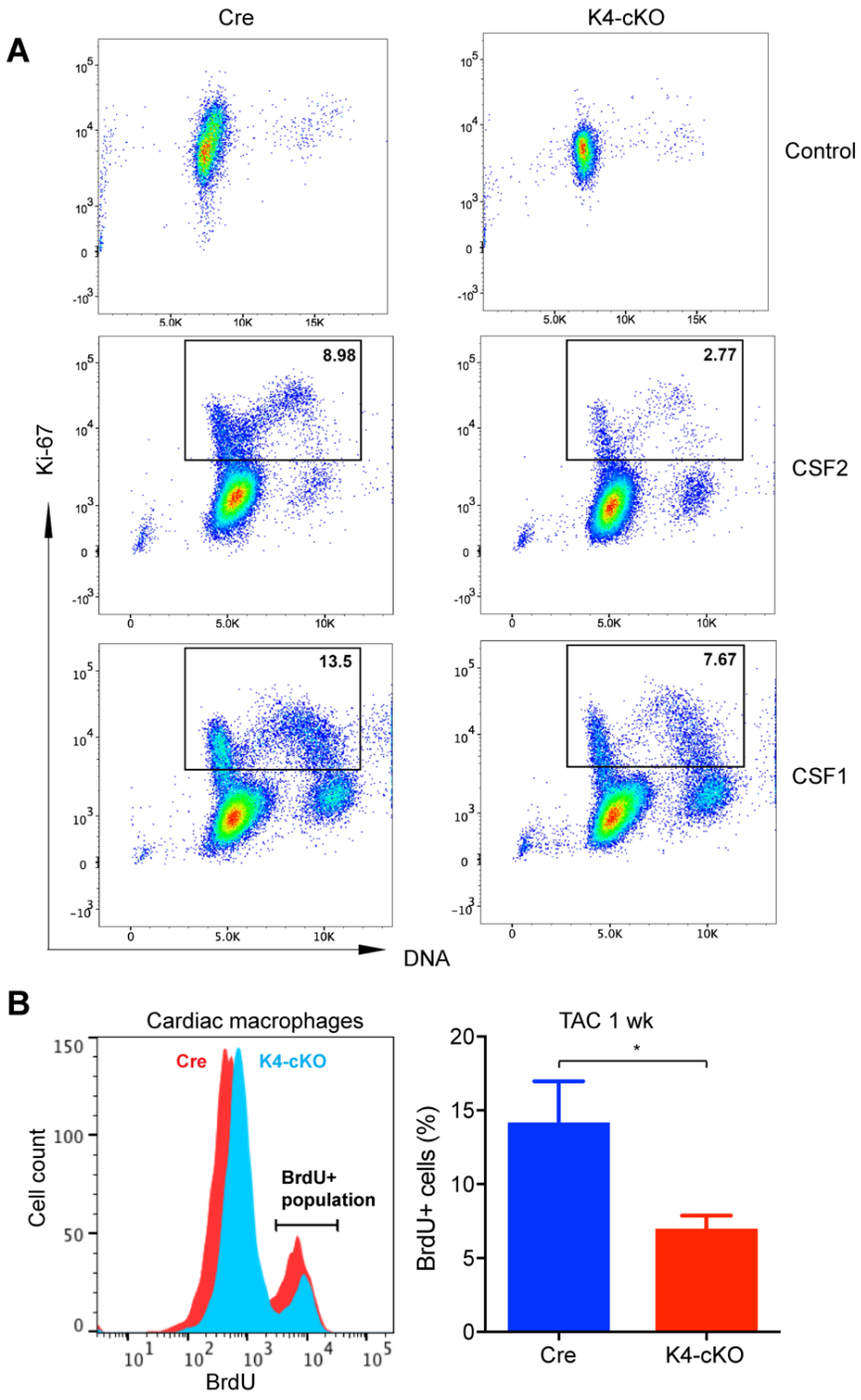

Figure S7. KLF4 deficiency impaired macrophage proliferation.

(A) Peritoneal macrophages isolated from Cre and K4-cKO mice were treated with CSF1 or CSF2 (10 ng/ml) for 48h before subjected to flow cytometry analysis for Ki-67 expression. DNA was stained by Hoeschst 33342. Gated cells were taken as Ki-67 positive populations. (B) BrdU-labelling in cardiac macrophages after 1-week TAC. *p<0.05 by t test. n=5.

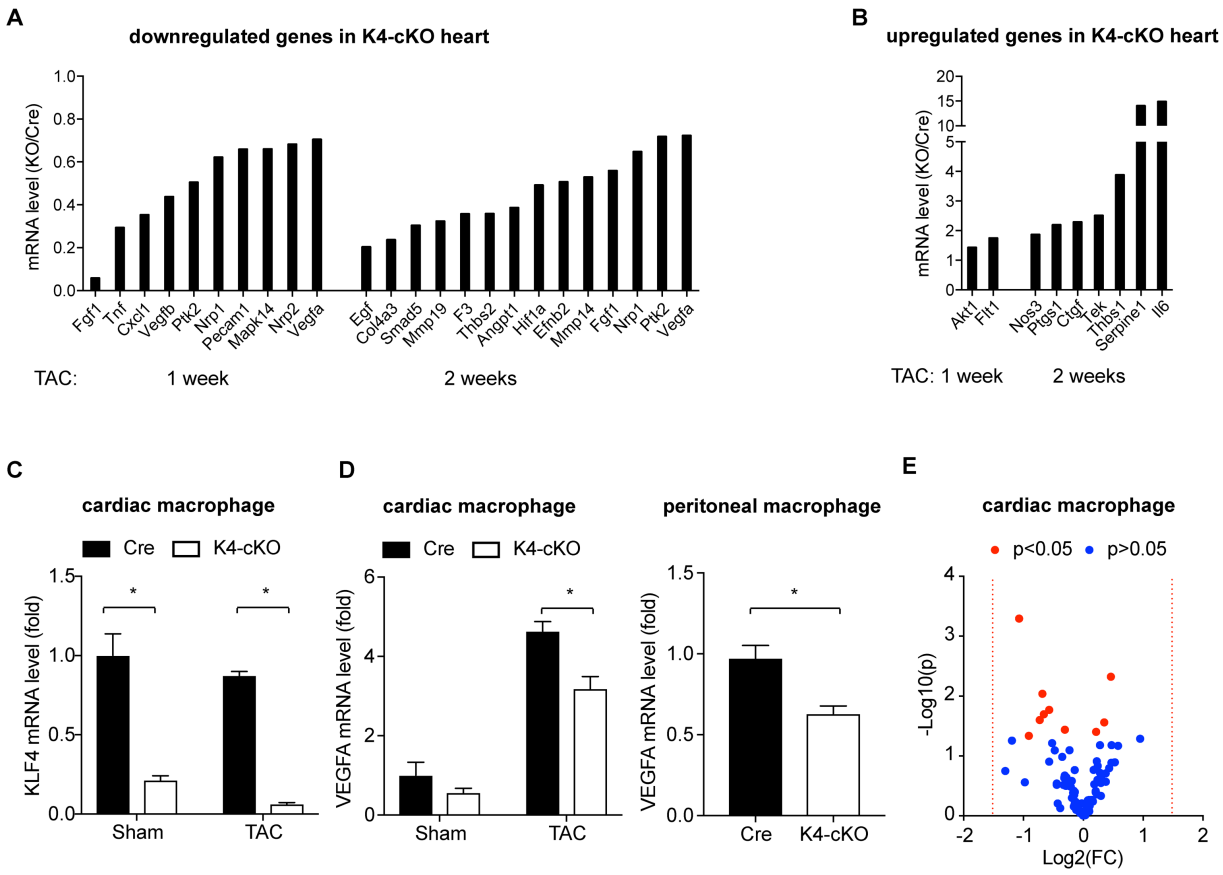

Figure S8. Myeloid KLF4 deficiency impaired angiogenesis.

(A, B) Expression of angiogenic genes in the heart before and after TAC. (C) KLF4 expression in cardiac macrophages isolated from Cre and K4-cKO mice at 1-week post-surgery. (D) VEGFA expression in peritoneal and cardiac macrophages. (E) Expression of 84 fibrosis genes in cardiac macrophages isolated from Cre and K4-cKO mice at 1-week post-TAC. There was no gene that had both a fold change (FC=KO/Cre) over ±1.5 (dotted red lines) and $p < 0.05$ (data point in red). For all data point, n=4 in each group, *p<0.05 between genotypes by t test with bonferroni correction.

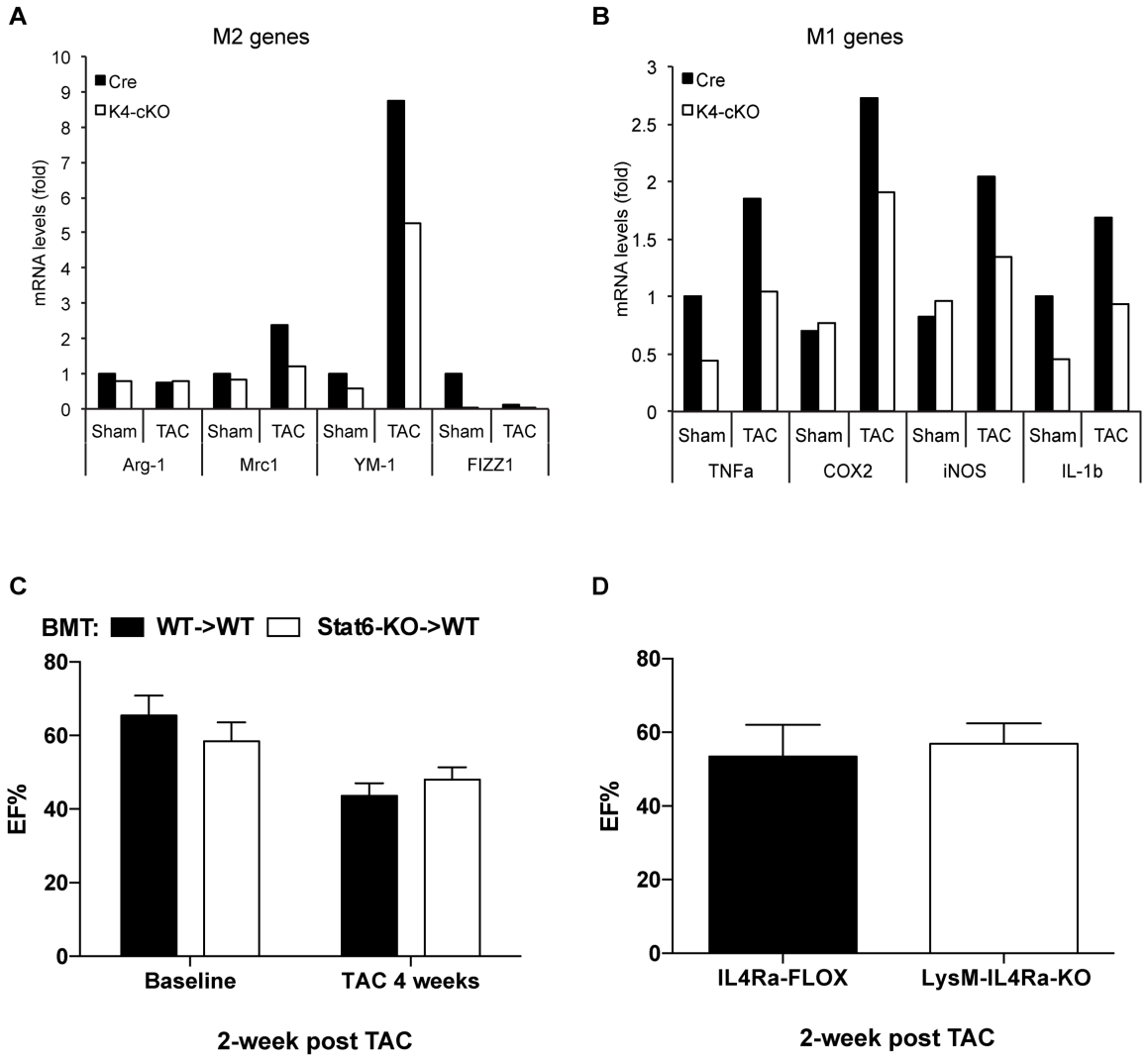

Figure S9. Deficiency of M2 macrophages did not affect POH.

(A, B) Expression of M1 and M2 genes in the Lyz2-Cre and K4-cKO hearts in response to TAC. (C, D) The IL4-Stat6 signaling pathway is a key regulator of macrophage M2 polarization but mice with either hematopoietic deficiency of Stat6 (C) or myeloid-specific deficiency of IL4 receptor (IL4Ra-KO) (D) exhibited normal cardiac responses to TAC. n=5.

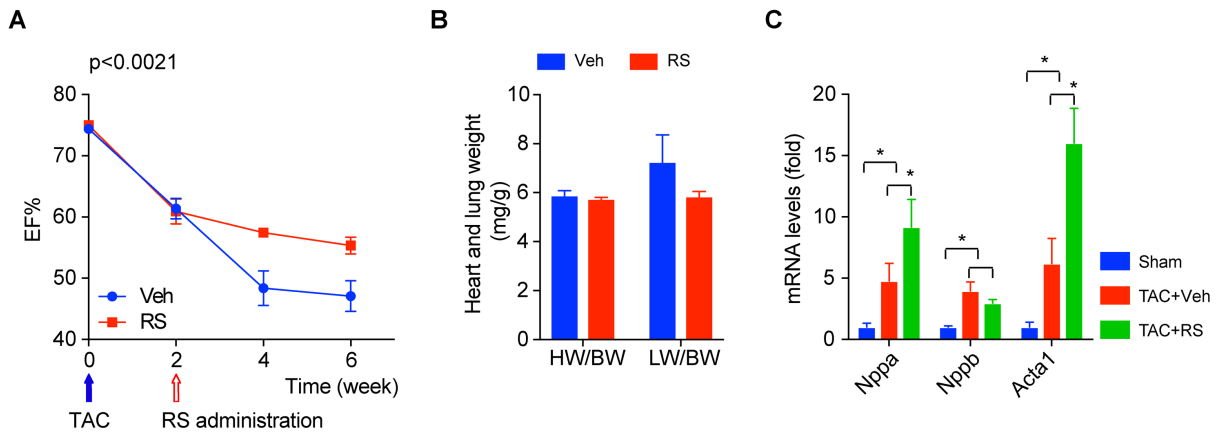

Figure S10. RS-504393 administration preserved cardiac function in established POH.

(A) LV function assessed by echocardiography. P value shown as P (treatment*time) calculated from Two-Way ANOVA. RS-504393 (RS) administration started from day-14 post-TAC to bypass the early adaptation phase. Arrows indicate treatment starting time. (B) Heart weight (HW) and lung weight (LW) normalized to body weight (BW). (C) Expression of hypertrophy marker genes. All tissue samples were assessed at 6-week post-TAC. n=6, *p<0.05 by t test with Bonferroni correction.